

# Acceleration signal in GRACE time-variable gravity in relation to interannual hydrological changes

Ryoko Ogawa,<sup>1,\*</sup> Benjamin F. Chao<sup>2,†</sup> and Kosuke Heki<sup>1</sup>

<sup>1</sup>Department of Natural History Sciences, Hokkaido University, Sapporo 060–0810, Japan

<sup>2</sup>Department of Earth Sciences, National Central University, Chung-Li 320, Taiwan, ROC. E-mail: bfchao@earth.sinica.edu.tw

Accepted 2010 October 5. Received 2010 July 22; in original form 2009 December 11

## SUMMARY

We use 6 yr of data of the GRACE (Gravity Recovery and Climate Experiment) satellite mission, which yield estimation for interannual signals in gravity changes. We solve for such signals in the form of not only linear trend but also quadratic term (acceleration/deceleration) of mass variations globally at a spatial resolution of 500 km. On continents they signify hydrological mass transport, where any linear trend in precipitation minus evapotranspiration is the input to and hence responsible for, the quadratic change in continental water storage and hence in gravity. Comparison studies of geographical patterns of the quadratic (representing acceleration/deceleration) terms show interesting agreement of the hydrological model GLDAS with GRACE data in many major areas, providing independent assessment as to the quality and validity of the hydrological models for interannual applications.

**Key words:** Satellite geodesy; Time variable gravity; Global change from geodesy; Hydrology.

## 1 INTRODUCTION

Many geophysical and climatic changes have been studied using time-variable gravity (TVG) data from the twin-satellite mission of Gravity Recovery and Climate Experiment (GRACE), which was launched in 2002. Subsequent to the first studies on seasonal hydrological cycles in the tropical regions (e.g. Tapley *et al.* 2004), some possibly long-term TVG trends began to be detected in various regions, for example, that due to present-day melting of ice sheet in the coastal Greenland (e.g. Luthcke *et al.* 2006) and of mountain glaciers in Alaska (e.g. Chen *et al.* 2006) and Asia (Matsuo & Heki 2010) and secular TVG increase by glacial isostatic adjustment (GIA) in northern North America (Tamisiea *et al.* 2007) and northern Europe (Steffen *et al.* 2009). In addition, interannual TVG indicated that the ice loss has been accelerating in Greenland (Velicogna & Wahr 2006) and in Antarctica (Chen *et al.* 2009).

With the accumulation of available GRACE TVG data in time span, it becomes imperative and feasible to begin to examine the temporal variation beyond the simple linear slope, which we refer to as ‘trend’ (during the studied time span). Such variation, for any given geographical location, constitutes by definition the longer-term acceleration (or deceleration) signal in TVG, which we shall simply model with a quadratic polynomial, or a parabolic function, of time within the studied time span. The acceleration in TVG naturally reflects the acceleration in the causes of TVG, that is, the mass transports in the Earth system. In particular, we shall

focus on the continental hydrological mass variations; any temporal acceleration thereof is obviously of grave importance in monitoring and understanding of present-day global climate change, as well as in predicting the future. Such is already the case in the case of the observed sea level rise, as emphasized in the Intergovernmental Panel on Climate Change 2007 report (Bindoff *et al.* 2007).

## 2 DATA AND PROCESSING

GRACE observations are processed at several research institutes. We use the Level-2 Release-04 data set from the University Texas Center for Space Research (Bettadpur 2007), given in the form of monthly spherical harmonic Stokes coefficients up to degree and order 60 ([http://podaac.jpl.nasa.gov/grace/data\\_access.html](http://podaac.jpl.nasa.gov/grace/data_access.html)). The data span 71 months from January 2003 to December 2008 (we exclude those in 2002 because of their poorer data quality). The  $C_{20}$  component, which represents the Earth’s varying oblateness but poorly determined by GRACE, is replaced with corresponding values derived from the Satellite Laser Ranging observations (Cheng & Ries 2007).

As GRACE data have rather serious short-wavelength and correlated errors, particularly the ‘striping’ noises, spatial filtering is necessary. In this paper, we apply the anisotropic fan filter which consists of low-pass filters along both the degree  $n$  and order  $m$  (Zhang *et al.* 2009), together with the de-correlation filter using polynomials of degree 4 for coefficients with  $m$  larger than 6 (Swenson & Wahr 2006).

For the TVG signals whose sources are mass transports occurring on the Earth’s surface, one can directly and uniquely convert the observed TVG into surface mass density changes (Chao 2005).

\*Now at: Schlumberger Middle East S.A.

†Now at: Institute of Earth Sciences, Academia Sinica, Taipei, Taiwan, ROC.

We do so in terms of the equivalent water thickness (EWT) to compare with meteorological quantities. In so doing we disregard any non-surface processes, which are not among the main interest of this paper, such as the GIA that would have hardly any quadratic acceleration signal.

Specifically, given the deviation from the static Stokes coefficients in terms of  $\Delta C_{nm}(t)$  and  $\Delta S_{nm}(t)$ , the EWT monthly map is constructed by the summation of spherical harmonics (Wahr *et al.* 1998; Chao 2005):

$$\Delta\sigma(\theta, \lambda, t) = \frac{a\rho_e}{3} \sum_{n=2}^{60} W_n \sum_{m=0}^n W_m \frac{(2n+1)}{(1+k_n)} \times P_{nm}(\cos\theta) [\Delta C_{nm}(t) \cos m\lambda + \Delta S_{nm}(t) \sin m\lambda], \quad (1)$$

where  $(\theta, \lambda) = (\text{colatitude, longitude})$ ,  $a$  and  $\rho_e$  are the equatorial radius and the mean density of the Earth, respectively and the load Love numbers  $k_n$  is to account for (or 'undo') Earth's elastic yielding effect under the mass loading in question.  $W_n, W_m$  are the fan filter weights; we chose Gaussian weight equivalent to 500 km filter length at Equator.

The EWT time series of any given location (or grid point on the global map) is then analysed to look for hydrological accelerations as follows. If the goal is to study the linear temporal trend in TVG, the common practice is to model the time series of each given location as:

$$\text{Mass}(t) = a_0 + a_1(t - t_0) + b_a \cos(\varpi t - \theta_a) + b_s \cos(2\varpi t - \theta_s), \quad (2)$$

where the last two terms represent the seasonal components (annual and semi-annual, respectively). The coefficient  $a_1$  is to account for any linear trend in mass variation over the observed period. Although the time derivative of the non-seasonal part of (2) does not mathematically depend on  $t$  or epoch  $t_0$ , different studied periods often yield different trends. For example (not shown here), such trend looks quite different between the first and the second halves of the time span in Eastern Europe; the increasing trend in the first half reverses itself in the second. The opposite is seen in equatorial Africa. In such cases, apparent trend changes can be part of the interannual variability or just a result of a couple of anomalous years, so a discussion on trend without specifying epoch is often inadequate, especially as the data time span increases.

Thus, to better account for possible temporal acceleration/deceleration, we add an additional quadratic term with coefficient  $a_2$  into expression (2):

$$\text{Mass}(t) = a_0 + a_1(t - t_0) + a_2(t - t_0)^2 + b_a \cos(\varpi t - \theta_a) + b_s \cos(2\varpi t - \theta_s). \quad (3)$$

Now the time derivative of eq. (3) depends on  $t$  and we need to specify epochs in addressing the trend. Note that the coefficient  $a_1$  represents the 'instantaneous' trend at the epoch  $t_0$ . Here we let epoch  $t_0 = 2006.0$ , the mid-point of our time span. In that case,  $a_1$  coincides with the average trend as recovered using eq. (2). The parameters in eq. (3) are estimated with the usual least-squares procedure. We plot the geographical distribution of the resultant values of the linear ( $a_1$  epoch  $t_0$ ) and quadratic ( $a_2$ ) coefficients for EWT in Figs 1(a) and (b), respectively.

GRACE data are known to suffer from the aliasing of tidal model errors (Ray & Luthcke 2006) and the  $K_2$  term may affect the estimation of quadratic signals with its relatively long aliasing period of 1362.7 d. We evaluated the shifts of the estimated quadratic terms by adding new terms changing with this period to eq. (3). We

confirmed that the  $K_2$  aliasing affects little the estimated quadratic terms.

While positive and negative quadratic terms show convex downward and upward time series, respectively, the interannual behaviour of time series depends on both linear and quadratic terms. For example, when  $a_1$  is positive, a positive (negative)  $a_2$  indicates acceleration (deceleration) of increase. However, when  $a_1$  is negative, a positive (negative)  $a_2$  would indicate deceleration (acceleration) of decrease. Thus, to avoid such ambiguities in the meaning of the simple words of acceleration or deceleration alone, we shall specify the polarity of the terms in each case as needed.

The statistical significance of the quadratic signal can be seen in the degree variance of the linear and quadratic terms (Fig. 2a). The estimated linear and quadratic terms remain well above formal uncertainties, scaled using post-fit residuals, up to degree 50. The coefficients with degrees  $>50$  have large uncertainties but they affect little the recovered gravity changes because of the application of the spatial filtering. Root-mean-square (rms) residual decreases as the number of estimated parameters increases with higher degree polynomials. Fig. 2(b) shows that this is the case and the rms decreases by adding the quadratic term exceeds those by adding any of the higher degree terms. Thus we confirm that modelling with quadratic function is statistically significant over modelling with just the linear trend during the time span we analysed, that is, the six full years of 2003–2008.

### 3 RESULTS AND DISCUSSIONS

Changes in the continental hydrological water storage in both forms of surface soil moisture and underground water are the main cause for (surface) TVG on land, which is observed by GRACE. Here we discuss possible origins of quadratic changes in water storage ( $W$ ), governed by the land-water budget equation:

$$\frac{dW}{dt} = P - E - R, \quad (4)$$

where  $P, E$  and  $R$  are the precipitation, evapotranspiration and runoff, respectively. If any of these fluxes contains a linear signal of the form  $\alpha t + \beta$ , it would translate into a quadratic signal in water storage:

$$W = \frac{1}{2}\alpha t^2 + \beta t + \text{const.} \quad (5)$$

Conversely, a quadratic signal in the water storage implies a linear trend in the combination of the three hydrological fluxes.

Thus, as a first experiment, let us first compare GRACE data with the linear trends in  $P$  estimated from meteorological data. Crowley *et al.* (2006) showed good agreements between groundwater changes from GRACE data and integrated monthly precipitation anomalies within the Congo Basin of Africa. Morishita & Heki (2008) compared  $P-E$  from meteorological data with anomalous changes in soil moisture related to El Niño/Southern Oscillation from GRACE data. Both studies integrate  $P$  or  $P-E$  to compare with  $W$  according to eq. (4) and assume constant  $R$  without better information. We, instead, directly compare linear trends in the both sides of eq. (4). The quantity  $dW/dt$  in eq. (4) can be obtained from GRACE data by calculating (i) monthly EWT at grid points as shown in eq. (1) and (ii) their month-to-month differences at these points. Then we could calculate its trend by estimating the linear term in the time series of  $dW/dt$  using eq. (2). This is equivalent to directly estimating the quadratic terms in GRACE with eq. (3) (Fig. 1b).

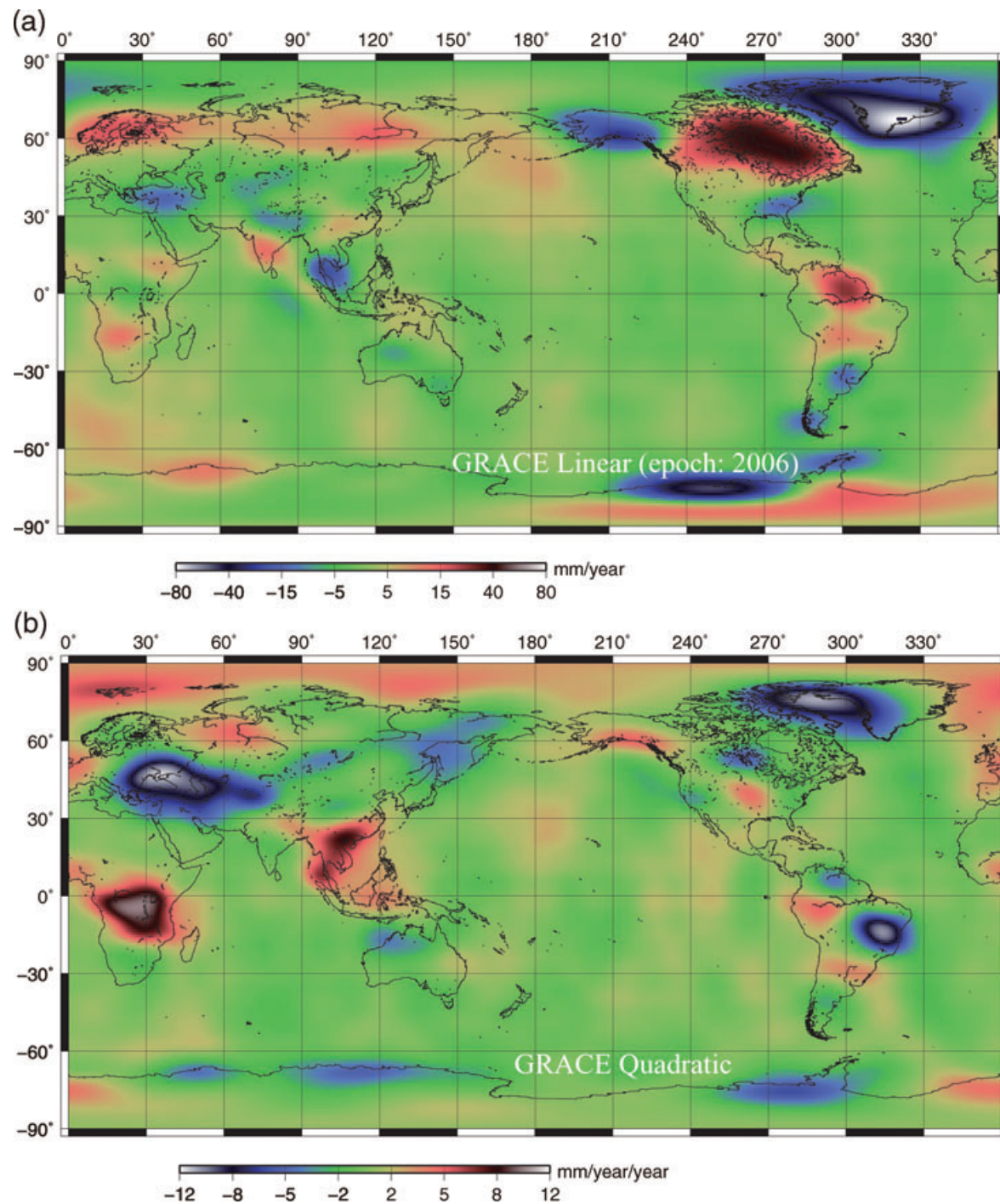


**Figure 1.** (a) Mean linear trend (epoch 2006.0) and (b) quadratic (acceleration/deceleration) of EWT from GRACE data, 2003–2008 (a 500-km fan filter and de-stripping filter applied).

In parallel, monthly worldwide precipitation data are available from CMAP (Climate Prediction Center Merged Analysis of Precipitation) at  $2.5 \times 2.5^\circ$  grids. CMAP provides merged precipitation data using rain gauge, satellite observation and NCEP (National Centers for Environmental Prediction) model output. We apply the same 500 km fan filter to allow direct comparison with the GRACE data. We then model  $P$  with eq. (2) to determine its linear trends and show them in Fig. 3 (the original value in mm/month/year of EWT is converted to those in mm/year/year to allow direct comparison

with Fig. 1b). These trends constitute the contribution of  $P$  to  $\beta$  in eq. (5).

When we compare Figs 1(b) and 3, both show clear systematic patterns in large areas of Africa, Eastern Europe, Siberia, Southeast Asia and central North America. It should be noted that the quantities shown in Fig. 3 should be twice as large as those in Fig. 1(b) as indicated by the factor 1/2 in eq. (5). However, the former is obviously larger than that, which is consistent with the fact that  $P$  is only the input of the hydrological budget that

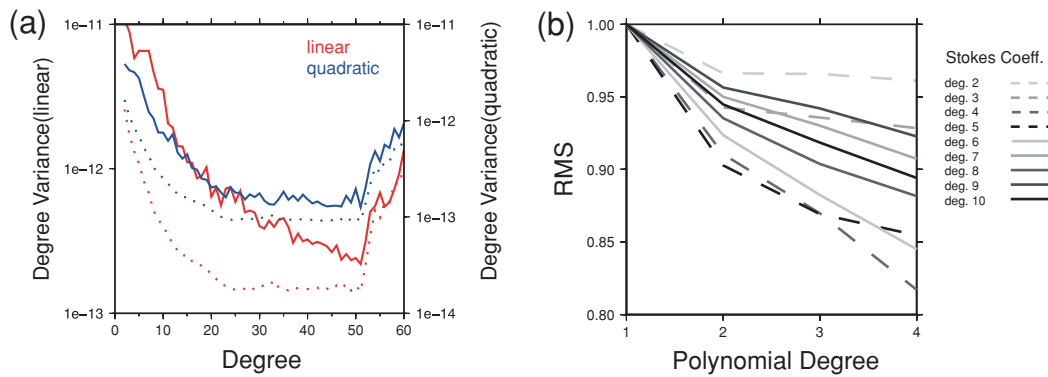


**Figure 2.** (a) Degree variance of linear and quadratic changes of GRACE TVG. Red and blue curves show linear and quadratic terms, respectively. They all exceed one-sigma errors shown with dotted curves. (b) Relationship between post-fit rms residuals of the Stokes coefficients of various spatial degrees and the polynomial degree for the assumed interannual fit (plus the seasonal terms). Residual decreases notably by adding the quadratic term (i.e. by changing polynomial degree from 1 to 2).

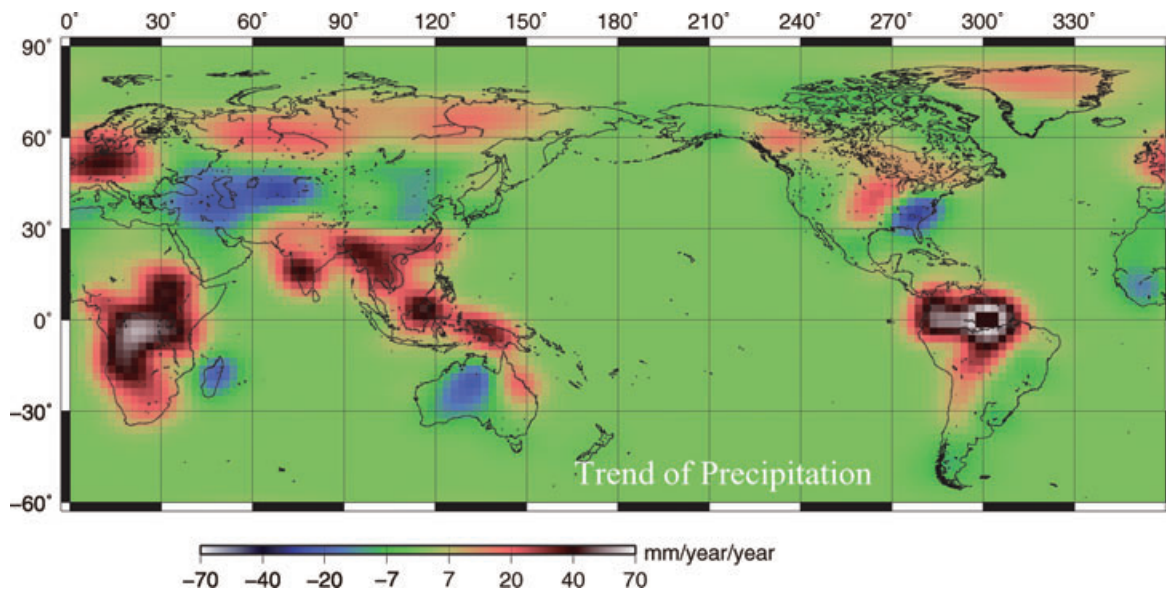


**Figure 3.** Linear trends in  $P$  from the CMAP meteorological data. The same spatial filters as the GRACE data have been applied.

determines  $dW/dt$  or  $W$  and one is still yet to take into account the water loss by  $E$  and  $R$  for a full comparison. Unfortunately, we find the latter not feasible at present. We have tried various ways to evaluate  $P-E$  or  $E$  alone from atmospheric general circulation model (GCM) data, for example using water balance in the atmosphere (Oki *et al.* 1995) or using temperature, hours of sunlight and precipitation data (Hamon 1963). They do agree well on the seasonal behaviour, but not on the linear trends over the studied period of time. Even when we use a same method on different atmospheric GCM output to evaluate  $P-E$ , the results for trends often disagree. Likewise is the model output for  $R$ ; at present their interannual behaviour does not close the water budget as dictated by eq. (4). Nevertheless, the point of comparing the spatial distribution of the trend of  $P$  with the quadratic changes in the GRACE data is simply to confirm readily that a direct relationship exists between them, the former as the source and the latter the consequence of the water budget.

To further validate the GRACE results with those from independent sources, we estimate the same parameters from the Global Land Data Assimilation System (GLDAS) Noah model (Rodell *et al.* 2004). GLDAS/Noah provides snow, canopy and soil mois-

ture data at  $1 \times 1^\circ$  grid points, except for Antarctica and Greenland where the hydrological condition is hardly subjective to modelling and the meteorological data are essentially unavailable. Although GLDAS terrestrial water changes in some regions show fairly good agreement with TVG from GRACE for their seasonal variations (Tapley *et al.* 2004, Syed *et al.* 2008), reliability of interannual changes in GLDAS hitherto have not been discussed sufficiently. Here we estimate linear and quadratic terms of terrestrial water storage from GLDAS data at grid points and apply the same 500 km fan filter as we did for GRACE data.

We can now compare linear signals of continental water storage in GLDAS (Fig. 4a) and GRACE (Fig. 1a) globally (except Antarctica and Greenland). The spatial pattern of the amplitude of GRACE and GLDAS linear trends agree fairly well in Africa, eastern North America, northern Australia and, to a lesser degree, near Amazon River and Siberia. Besides, GRACE shows larger negative trend in Alaska, Patagonia, Asian high mountains than GLDAS, presumably because the latter does not include the recent melting of mountain glaciers. GLDAS also shows poor agreement in northern India with GRACE because GLDAS does not simulate changes in groundwater (e.g. Rodell *et al.* 2009). GRACE data, however, also include



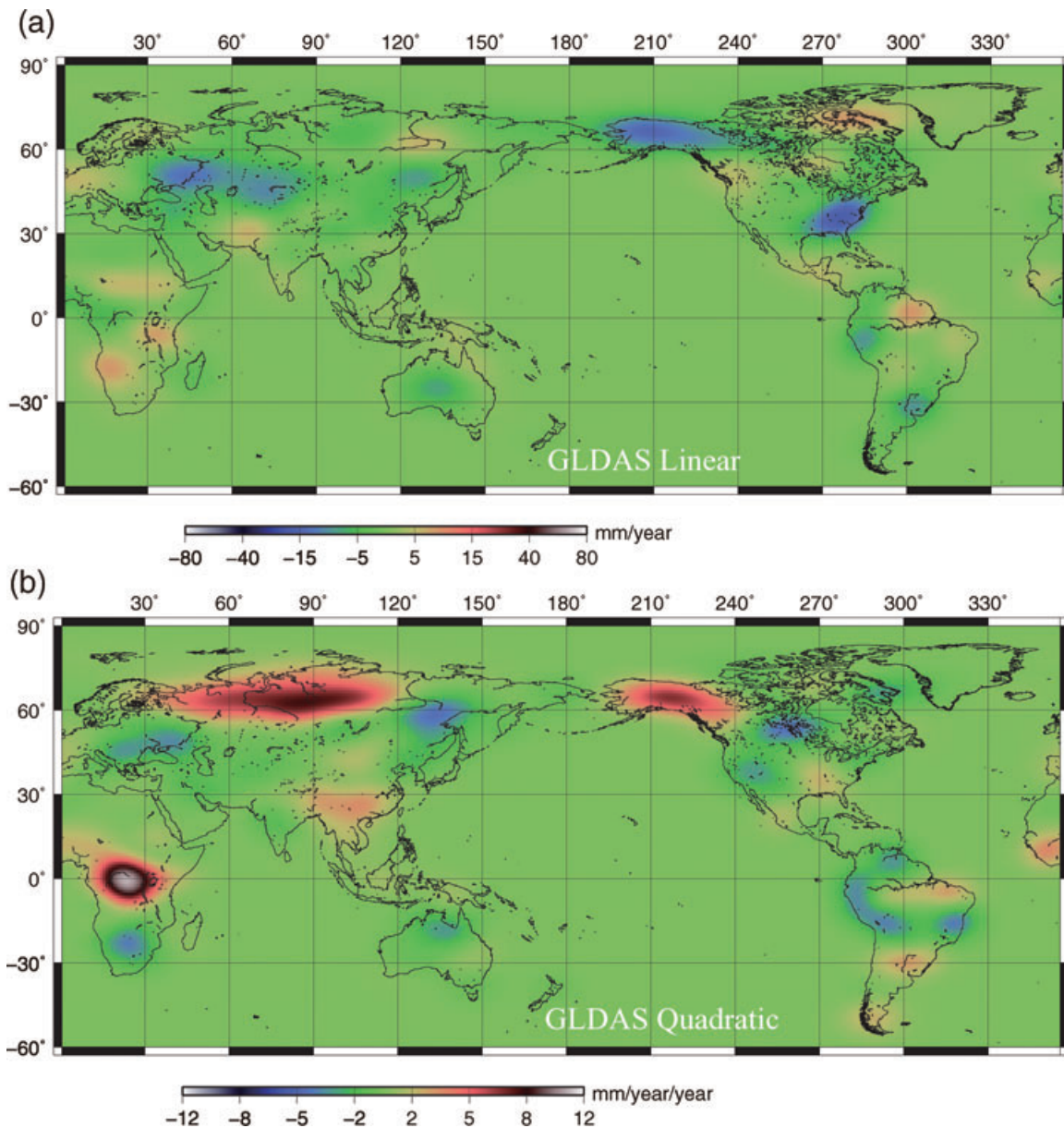


**Figure 4.** Same as Fig. 1, but for the GLDAS hydrological model output. Greenland and Antarctica are excluded.

non-hydrological gravity changes, for example, GIA signals as in Northern Canada and Scandinavia and co-seismic and post-seismic gravity changes of the great 2004 Sumatra–Andaman earthquake (e.g. Han *et al.* 2006; Ogawa & Heki 2007).

Next we compare Figs 1(b) and 4(b) for the quadratic signal. We see interesting, and sometimes remarkable, agreement in the patterns of GRACE and GLDAS in many major areas. Positive quadratic signals (in red) are seen in both cases in equatorial Africa, Southeast Asia, western Siberia and to a lesser extent in central North America and Alaska. Similarly, negative quadratic signals (in blue) are seen in both cases in Eastern Europe and Southern South America. On the other hand, we note that their amplitudes are somewhat different, with larger differences tending to be in regions near major rivers. In the present case, the anomalies in  $P$  lead to and hence are largely offset by, opposite changes in  $R$  mainly via rivers and partly via groundwater storage; the time constant of the latter is much longer than the former. As the nominal depth

of soil layers treated in GLDAS/Noah model is 2 m, groundwater is not considered in its output. The present result suggests that the groundwater plays a non-negligible role in regulating  $W$  on not only linear but also quadratic signals as suggested in Rodell & Famiglietti (2001) and Rodell *et al.* (2007).

For a case study in more detail, we focus on Eastern Europe in the comparison between Figs 1(b) and 4(b), where the GRACE quadratic signal much exceeds that of GLDAS. The observed large negative quadratic signals by GRACE would be due to the leakage from ocean mass changes. Generally speaking, long-term gravity changes in oceanic areas are much smaller than those on land. Relatively small oceans surrounded by continents, however, might show signals comparable to land regions. For example, both GRACE and altimetry detected relatively large seasonal signals in the Mediterranean Sea (Garcia *et al.* 2006).

In fact, Swenson & Wahr (2007) showed a positive trend in GRACE gravity in the Caspian Sea up to 2006. Thus, we also analyse

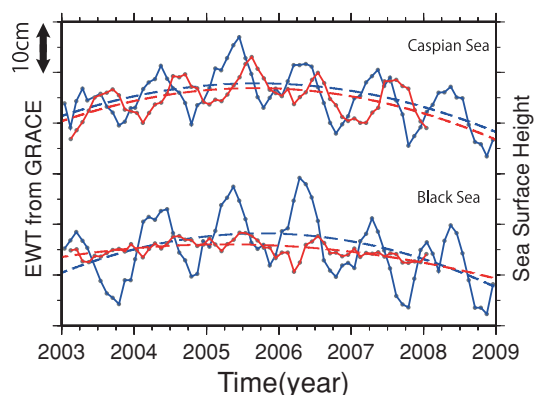


**Figure 5.** Time series of EWT in the Caspian Sea (top) and the Black Sea (bottom). Blue curves show mass change from GRACE gravity data in the two seas. Red curves show corrected sea surface height from AVISO at arbitrary points in these seas. Dashed curves show best-fit quadratic functions.

mass changes in the Caspian and Black Seas using 2003–2008 GRACE data with ‘boxcar’ land masks. In both seas, EWT shows increases up to 2005, but reverted to decreases after 2006 (Fig. 5, blue curves). Indeed, precipitation decreases linearly in the whole regions during the period (Fig. 3).

These changes of precipitation should also be seen in the sea surface height (SSH). Therefore, we make use of the satellite ocean altimetry data from AVISO (Archiving, Validation and Interpretation of Satellite Oceanographic data; <http://www.aviso.oceanobs.com/en/data/products/sea-surface-height-products/global/index.html>) to compare directly with GRACE quadratic changes. To do so, we multiply an empirical factor to the SSH in accordance with Swenson & Wahr (2007). Of course we do not expect them to agree because GRACE data only reflect the mass variation while the altimetry gives the total SSH which also includes the steric contribution. Nevertheless, similar negative quadratic signal is also present in the altimetry data for the Caspian Sea. The Black sea SSH shows similar but weaker negative quadratic signal. Amplitude of its seasonal change is also significantly smaller than those in GRACE. The Caspian Sea, being a closed water basin, would have accumulated, or integrated, such trend more effectively than did the Black Sea, which is connected (although indirectly) to the global ocean.

#### 4 CONCLUSIONS

With 6 yr of GRACE data, we find that the quadratic variation of TVG is significant both in wavenumber and space domains. Quadratic terms are significant in many regions, including equatorial Africa, Eastern Europe, central North America, Southeast Asia and Amazon basin; the actual behaviour in terms of acceleration or deceleration of increases or decreases is to be determined by a combined interpretation of the linear trend and the quadratic term given in Figs 1(a) and (b).

The quadratic variations are indicative particularly of interannual changes in terrestrial water storage  $W$ . Comparison with meteorological data suggests that the trends of precipitation  $P$  have similar distribution to  $W$  according to GRACE although we still lack accurate knowledge of interannual changes in evapotranspiration  $E$  and runoff  $R$  to study  $W$  fully. Nevertheless, we confirm that the quadratic term in TVG would be a manifestation of linear trend of  $P$ . Hydrological model GLDAS, which includes  $E$  and  $R$ , also shows

geographical patterns of linear and quadratic changes in agreement with those of GRACE in many major areas.

GLDAS/Noah model tends to underestimate the interannual changes of  $W$ , presumably because it does not currently simulate changes in groundwater and surface water storages. The comparison indicates for the first time that both the GRACE observation and the GLDAS hydrological model are capturing the interannual variability by yielding qualitatively ‘correct’ estimates for interannual mass variations. Full comparison with hydrological models needs further investigations, especially on interannual behaviours of groundwater storage. On the other hand, further quantitative comparison of the quadratic (acceleration/deceleration) terms can provide independent assessment as to the quality and validity of the hydrological models for interannual applications.

#### ACKNOWLEDGMENTS

We thank two anonymous reviewers for constructive comments and Dr. Zi-Zhan Zhang for discussions. This work is supported in part by the National Science Council of Taiwan and Grant-in-Aid for JSPS (Japanese Society for Promotion of Science) Fellows during the tenure of the first authors (RO) in the National Central University in Taiwan.

#### REFERENCES

- Bettadpur, B., 2007. CSR level-2 processing standards document for product release 04 GRACE, CSR Publ. GR-03-03, 327–742, University of Texas at Austin, Austin, TX, 17pp.
- Bindoff, N.L. *et al.*, 2007. In *Climate Change 2007: The Physical Science Basis*, in *Contribution of Working Group I to the Fourth Assessment Report of the Intergovernmental Panel on Climate Change*, Chapter 5, Cambridge University Press, New York.
- Chao, B.F., 2005. On inversion for mass distribution from global (time-variable) gravity field, *J. Geodyn.*, **39**, 223–230, doi:10.1016/j.jog.2004.11.001.
- Chen, J.L., Tapley, B.D. & Wilson, C.R., 2006. Alaskan mountain Glacial melting observed by Satellite gravimetry, *Earth planet. Sci. Lett.*, **248**, 368–378, doi:10.1016/j.epsl.2006.05.039.
- Chen, J.L., Wilson, C.R., Blankenship, D. & Tapley, B.D., 2009. Accelerated Antarctic ice loss from satellite gravity measurements, *Nat. Geosci.*, **2**, doi:10.1038/ngeo694.
- Cheng, M. & Ries, J., 2007. GRACE technical note no.5: monthly estimates of  $C_{20}$  from 5 SLR satellites, <http://podaac.jpl.nasa.gov/grace/documentation.html> (last accessed 2009 December 11).
- Crowley, J.W., Mitrovica, J.X., Bailey, R.C., Tamisiea, M.E. & Davis, J.L., 2006. Land water storage within the Congo Basin inferred from GRACE satellite gravity data, *Geophys. Res. Lett.*, **33**, L19402, doi:10.1029/2006GL027070.
- García, D., Chao, B.F., Del Río, J., Vigo I. & García-Lafuente, J., 2006. On the steric and mass-induced contributions to the annual sea level variations in the Mediterranean Sea, *J. geophys. Res.*, **111**, C09030, doi:10.1029/2005JC002956.
- Hamon, R.W., 1963. Computation of direct runoff amounts from storm rainfall, *Int. Assoc. Sci. Hydrology*, **63**, 52–62.
- Han, S.C., Shum, C.K., Bevis, M., Ji, C. & Kuo, C.Y., 2006. Crustal dilatation observed by GRACE after the 2004 Sumatra-Andaman earthquake, *Science*, **313**, 658–666, doi:10.1126/science.1128661.
- Luthcke, S.B. *et al.*, 2006. Recent Greenland ice mass loss by drainage system from satellite gravity observations, *Science*, **314**, 1286–1289, doi:10.1126/science.1130776.
- Matsuo, K. & Heki, K., 2010. Time-variable ice loss in Asian high mountains from satellite gravimetry, *Earth planet. Sci. Lett.*, **290**, 30–36, doi:10.1016/j.epsl.2009.11.053.
- Morishita, Y. & Heki, K., 2008. Characteristic precipitation patterns of El Niño/La Niña in time-variable gravity fields by GRACE, *Earth planet. Sci. Lett.*, **272**, 677–682, doi:10.1016/j.epsl.2008.06.003.

- Ogawa, R. & Heki, K., 2007. Slow postseismic recovery of geoid depression formed by the 2004 Sumatra-Andaman Earthquake by mantle water diffusion, *Geophys. Res. Lett.*, **34**, L06313, doi:10.1029/2007GL029340.
- Oki, T., Musiak, K., Matsuyama, H. & Masuda, K., 1995. Global atmospheric water balance and runoff from large river basins, *Hydrol. Proc.*, **9**, 655–678, doi:10.1002/hyp.3360090513.
- Ray, R.D. & Luthcke, S.B., 2006. Tide model errors and GRACE gravimetry: towards a more realistic assessment, *Geophys. J. Int.*, **167**, 1055–1059, doi:10.1111/j.1365-246X.2006.03229.x.
- Rodell, M. & Famiglietti, J.S., 2001. An analysis of terrestrial water storage variations in Illinois with implications for the gravity recovery and climate experiment (GRACE), *Water Resour. Res.*, **37**, 1327–1339.
- Rodell, M. *et al.*, 2004. The Global Land Data Assimilation System, *Bull. Am. Meteorol. Soc.*, **85**, 381–394.
- Rodell, M., Chen, J., Kato, H., Famiglietti, J.S., Nigro, J. & Wilson, C.R., 2007. Estimating groundwater storage changes in the Mississippi River basin (USA) using GRACE, *Hydrogeol. J.*, **15**, 159–166.
- Rodell, M., Velicogna, I. & Famiglietti, J.S., 2009. Satellite-based estimates of groundwater depletion in India, *Nature*, **460**, 999–1002.
- Steffen, H., Gitlein, O., Denker, H., Muller, J. & Timmen, L., 2009. Present rate of uplift in Fennoscandia from GRACE and absolute gravimetry, *Tectonophysics*, **474**, 69–77, doi:10.1016/j.tecto.2009.01.012 474.
- Swenson, S. & Wahr, J., 2006. Post-processing removal of correlated errors in GRACE data, *Geophys. Res. Lett.*, **33**, L08402, doi:10.1029/2005GL025285.
- Swenson, S. & Wahr, J., 2007. Multi-sensor analysis of water storage variations of the Caspian Sea, *Geophys. Res. Lett.*, **34**, L16401, doi:10.1029/2007GL030733.
- Syed, T.H., Famiglietti, J.S., Rodell, M., Chen, J. & Wilson, C.R., 2008. Analysis of terrestrial water storage changes from GRACE and GLDAS, *Water Resour. Res.*, **44**, W02433, doi:10.1029/2006WR005779.
- Tamisiea, M. E., Mitrovica, J.X. & Davis, J.L., 2007. GRACE gravity data constrain ancient ice geometries and continental dynamics over Laurentia, *Science*, **316**, 881–883, doi:10.1126/science.1137157.
- Tapley, B.D., Bettadpur, S., Ries, J.C., Thompson, P.F. & Watkins, M.M., 2004. GRACE measurements of mass variability in the earth system, *Science*, **305**, 503–505, doi:10.1126/science.1099192.
- Velicogna, I. & Wahr, J., 2006. Acceleration of Greenland ice mass loss in spring 2004, *Nature*, **443**, 329–331, doi:10.1038/nature05168.
- Wahr, J., Molenaar, M. & Bryan, F., 1998. Time variability of the Earth's gravity field: hydrological and oceanic effects and their possible detection using GRACE, *J. geophys. Res.*, **103**, 30 205–30 229.
- Zhang, Z.Z., Chao, B.F., Lu, Y. & Hsu, H.T., 2009. An effective filtering for GRACE time-variable gravity: fan filter, *Geophys. Res. Lett.*, **36**, L17311, doi:10.1029/2009GL039459.